Journal of Solid State Chemistry 181 (2008) 3303–3307

Contents lists available at ScienceDirect

Journal of Solid State Chemistry

journal homepage: www.elsevier.com/locate/jssc

NMR evidence of LiF coating rather than fluorine substitution in $Li(Ni_{0.425}Mn_{0.425}Co_{0.15})O_2$

M. Ménétrier [a], J. Bains [a], L. Croguennec [a,*], A. Flambard [a], E. Bekaert [a], C. Jordy [b], Ph. Biensan [b], C. Delmas [a]

[a] ICMCB, CNRS, Université Bordeaux 1, Site ENSCPB, 87 avenue Schweitzer, 33608 PESSAC cedex, France
[b] SAFT, Direction de la Recherche, 111-113 Bld Alfred Daney, 33074 Bordeaux, France

ARTICLE INFO

Article history:
Received 16 April 2008
Received in revised form
28 August 2008
Accepted 1 September 2008
Available online 18 September 2008

Keywords:
Lithium-ion battery
Positive electrode material
Layered oxide
$Li(Ni,Mn,Co)O_2$
Fluorine substitution
Coating
X-ray diffraction
NMR spectroscopy

ABSTRACT

A series of "$Li_{1+z/2}(Ni_{0.425}Mn_{0.425}Co_{0.15})_{1-z/2}O_{2-z}F_z$" materials was prepared by a coprecipitation route and their structure was characterized using X-ray diffraction (XRD), as well as ^7Li and ^{19}F Magic Angle Spinning (MAS) NMR spectroscopy. Two hypotheses were considered: (i) formation of layered oxyfluoride materials and (ii) formation of a mixture between the layered material and LiF. Structural parameters were refined by the Rietveld method, using XRD diffraction data. The refinement results did not allow us to choose between these two hypotheses: no significant change in crystallinity and structural parameters was observed irrespective of the fluorine ratio. ^7Li and ^{19}F MAS NMR analyses showed signals with isotropic positions characteristic of LiF, but envelopes characteristic of very strong dipolar interactions with the electron spins of the material, demonstrating that LiF was not incorporated into the layered oxide structure but was instead present as a coating.

1. Introduction

Currently, $LiCoO_2$ is the most widely used positive electrode material in commercial lithium-ion batteries. However, because of its high cost and limited cyclability and chemical stability at high voltage, various partial substitutions for Ni in $LiNiO_2$ were investigated [1–7]. Recently, $Li_{1+x}(Ni_yMn_yCo_{1-2y})_{1-x}O_2$ systems have been suggested to be the most promising alternative to $LiCoO_2$ [8–12]. These systems consist of $Ni^{2+,\ 3+}$, Mn^{4+} and Co^{3+} ions. Mn^{4+} is electrochemically inactive so that it provides significant structural stability during electrochemical cycling (no detrimental effect of the Jahn–Teller distortion associated with Mn^{3+}), while Ni^{2+} and Co^{3+} are electroactive through $Ni^{2+/3+/4+}$ and $Co^{3+/4+}$ redox couples [9,13,14]. The electrochemical performance of the $Li(Ni_{1/3}Mn_{1/3}Co_{1/3})O_2$ system was found to be highly dependent on the current density and cut-off voltage, with a rather fast reversible capacity fading when cycling is, for instance, performed in a large potential window [15]. In order to improve the electrochemical performance, two approaches were developed: (i) ionic substitution to increase the structural stability of the layered oxide [16–19] and (ii) surface modification to stabilize the layered oxide surface through an impedance decrease [20]. The LiF addition to $Li_{1+x}(Ni_yMn_yCo_{1-2y})_{1-x}O_2$ materials was shown to improve their cycling performance and thermal stability [21]. But conflicting explanations are proposed in the literature: most of the authors considered that fluorine substitution for oxygen is effective since changes in cell parameters were, for instance, observed using X-ray diffraction (XRD) [22–25], while others recently showed by XPS analyses that fluorine exists as an LiF surface layer [26].

In this paper, we report attempts for the synthesis of "$Li_{1+z/2}(Ni_{0.425}Mn_{0.425}Co_{0.15})_{1-z/2}O_{2-z}F_z$" materials by the coprecipitation route. Their structural properties have been studied by XRD and NMR spectroscopy. The aim of this paper was to determine whether fluoride ions are actually incorporated within the layered lattice.

2. Experimental

A series of materials with nominal "$Li_{1+z/2}(Ni_{0.425}Mn_{0.425}Co_{0.15})_{1-z/2}O_{2-z}F_z$" ($z = 0,\ 0.1,\ 0.2$) compositions was prepared following the solid-state syntheses reported by Kim et al. [22,23] using LiF as the fluorine precursor. The first step of the synthesis consisted in the formation of $Li(Ni_{0.425}Mn_{0.425}Co_{0.15})O_2$ using the coprecipitation route and then in the addition of LiF aiming the

* Corresponding author. Fax: +33 5 4000 2761.
E-mail address: laurence.croguennec@icmcb-bordeaux.cnrs.fr (L. Croguennec).

0022-4596/$ - see front matter © 2008 Elsevier Inc. All rights reserved.
doi:10.1016/j.jssc.2008.09.002

target stoichiometry $Li_{1+z/2}(Ni_{0.425}Mn_{0.425}Co_{0.15})_{1-z/2}O_{2-z}F_z$. A mixed (1 M) aqueous solution of $Ni(NO_3)_2 \cdot 6H_2O$ (98% Prolabo), $Mn(NO_3)_2 \cdot 4H_2O$ (98% Prolabo) and $Co(NO_3)_2 \cdot 6H_2O$ ($\geqslant$98% Fluka), prepared with the 42.5/42.5/15 Ni/Mn/Co molar ratio, was added dropwise into a basic solution (LiOH 1 M (98% Alfa Aesar)/NH_4OH 3 M (28% Prolabo)) under magnetic stirring. The nominal Li/*M* ratio was adjusted to 1.02 to compensate for lithium loss due to the high temperature of the synthesis (*M* being for transition metal ions). A green–brown mixed hydroxide precipitated. Water was evaporated at 80 °C under primary vacuum using a rotavapor device. The resulting precipitate was dried overnight in an oven at 105 °C; then it was heated in air in a tubular furnace up to 500 °C for 5 h to decompose nitrates and finally calcinated in air at 900 °C for 12 h (heating and cooling rates: 2 °C/min). As described just after, the $Li(Ni_{0.425}Mn_{0.425}Co_{0.15})O_2$ phase was characterized in detail by XRD and an ICP titration before being used as a precursor for the synthesis of the fluorinated phases. The second step consisted of mixing in an agate mortar the prepared $Li(Ni_{0.425}Mn_{0.425}Co_{0.15})O_2$ powder with LiF powder (99.9% Prolabo) according to the chemical equation: $1-z/2\ Li(Ni_{0.425}Mn_{0.425}Co_{0.15})O_2 + z\,LiF \rightarrow Li_{1+z/2}(Ni_{0.425}Mn_{0.425}Co_{0.15})_{1-z/2}O_{2-z}F_z$ ($z = 0, 0.1, 0.2$). The resulting mixture was heated in a gold crucible in air at 875 °C for 5 h (heating and cooling rates: 2 °C/min) and finally ground in an agate mortar. According to these expected chemical formulae $Li_{1+z/2}(Ni_{0.425}Mn_{0.425}Co_{0.15})_{1-z/2}O_{2-z}F_z$, irrespective of the *z* value, the average oxidation state of the transition metal ions is expected to remain equal to 3. Indeed, the only fluorine substitution for oxygen would theoretically lead to the reduction of *M* according to ($1O^{2-}+1M^{3+} \equiv 1F^{-}+1M^{2+}$). Nevertheless, in $Li_{1+z/2}(Ni_{0.425}Mn_{0.425}Co_{0.15})_{1-z/2}O_{2-z}F_z$ the presence of extra-lithium ions—that would be theoretically compensated by the oxidation of *M* ions ($3M^{3+} \equiv 1Li^{+}+2M^{4+}$)—leads in fact to charge compensation without any modification of the transition metal ion oxidation state (as $\frac{1}{2}M^{3+}+1O^{2-} \equiv \frac{1}{2}Li^{+}+1F^{-}$).

The average oxidation state of the transition metal ions was determined by iodometric titration with $Na_2S_2O_3$. Lithium and transition metal ions were titrated using ICP measurements (Thermo Iris Interpid II XP). Synthesized powders were solubilized in an acidic solution. Fluorine and transition metal ions were titrated using an electron microprobe (CAMECA SX 100). Powders were pressed into $\varnothing$13 mm pellets and metallized by gold–palladium plasma.

Powder XRD analyses were performed using a Siemens D5000 diffractometer and Cu$K\alpha$ radiation. The diffraction patterns were recorded in the 10–80° (2θ) range using 0.02° (2θ) step of a 2 s duration for routine characterization. For structural study using the Rietveld method, data were collected in the 5–120° (2θ) range with steps of 0.02° (2θ) and a constant counting time of 8 s.

Materials were characterized by ^7Li and ^{19}F MAS NMR at 116.6 and 282.4 MHz, respectively, using an Avance 300 MHz Bruker spectrometer and a (90–τ–180) rotor-synchronized Echo-MAS sequence (30 kHz spinning speed). The ^7Li and ^{19}F chemical shifts were externally referenced to LiCl (1 M) and $CFCl_3$ at 0.0 ppm, respectively.

3. Results and discussion

3.1. Structural characterization: XRD analyses

The XRD patterns of "$Li_{1+z/2}(Ni_{0.425}Mn_{0.425}Co_{0.15})_{1-z/2}O_{2-z}F_z$" materials are compared in Fig. 1. Unexpectedly, these three diffraction patterns are very similar irrespective of the fluorine ratio ($z = 0$, 0.1 and 0.2). All the diffraction peaks could be indexed in the $R\bar{3}m$ space group: no extra peaks associated with LiF could be observed. According to XRD, pure α-$NaFeO_2$-type phases are thus obtained. The widths of the diffraction lines are very similar for the three materials. The full widths at half maximum (FWHM) of the (003) and (104) diffraction lines are about 0.10° and 0.16°, respectively, with an intensity ratio $I_{(003)}/I_{(104)}$ close to 1.06. The splitting of the (018)/(110) doublet is also very similar for the three materials.

The chemical composition of the resulting powders was analyzed by the ICP titration and microprobe. The experimental results were found to be in very good agreement with the nominal compositions (Table 1) and redox titration showed an average oxidation state of the transition metal close to 3; we thus considered the nominal compositions for the refinements of the XRD data by the Rietveld method.

XRD patterns were first analyzed by full pattern matching: only the cell and the profile function parameters were refined. The profile function was described by a pseudo-Voigt and the profile function parameters were found to remain almost constant with increasing fluorine substitution ($U \sim 0.11$, $V \sim 0.03$ and $W \sim 0.002$).

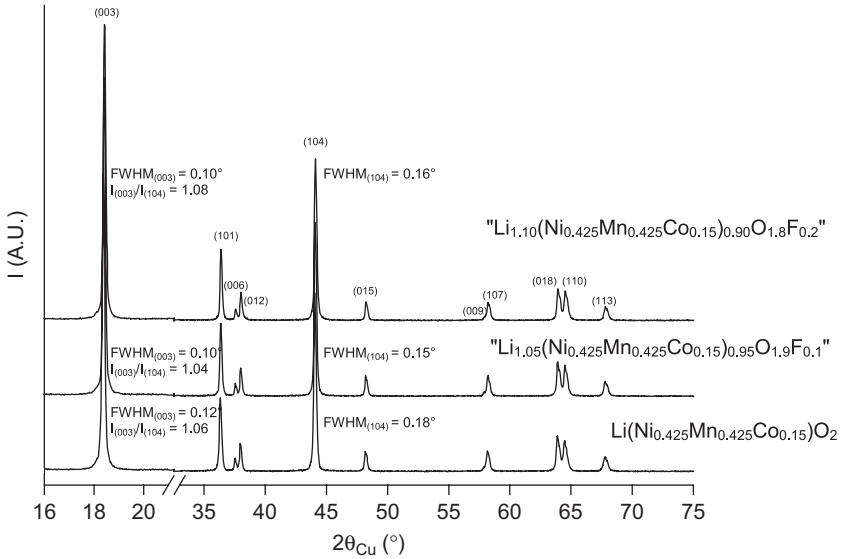

Fig. 1. XRD patterns of the "$Li_{1+z/2}(Ni_{0.425}Mn_{0.425}Co_{0.15})_{1-z/2}O_{2-z}F_z$" samples prepared by coprecipitation.

Table 1
Results of the chemical and redox analyses for the "$Li_{1+z/2}(Ni_{0.425}Mn_{0.425}Co_{0.15})_{1-z/2}O_{2-z}F_z$" samples ($z = 0$, 0.1, 0.2) obtained by iodometric and ICP titrations and microprobe analyses

Material	Oxid. state	ICP analysis				Microprobe analysis	
		$(Li/M)_{th.}$	$(Li/M)_{exp.}$	$(Ni/Mn)_{exp.}$	$(Co/Mn)_{exp.}$	$(F/M)_{th.}$	$(F/M)_{exp.}$
$Li(Ni_{0.425}Mn_{0.425}Co_{0.15})O_2$	3.02	1.00	1.04	0.98	0.34	0	0
"$Li_{1.05}(Ni_{0.425}Mn_{0.425}Co_{0.15})_{0.95}O_{1.9}F_{0.1}$"	3.03	1.11	1.15	1.01	0.35	0.11	0.09
"$Li_{1.10}(Ni_{0.425}Mn_{0.425}Co_{0.15})_{0.90}O_{1.8}F_{0.2}$"	3.02	1.22	1.26	1.02	0.35	0.22	0.15

Table 2
Structural parameters determined for "$Li_{1+z/2}(Ni_{0.425}Mn_{0.425}Co_{0.15})_{1-z/2}O_{2-z}F_z$" ($z = 0$, 0.1, 0.2) by the refinement of their X-ray diffraction data by the Rietveld method

Material	Hyp. (*)	a_{hex} (Å)	c_{hex} (Å)	V (Å^3)	z(O,F)$_{6c}$	Occ(Ni$_{3b}$)	R_{wp} (%)	R_B (%)
$Li(Ni_{0.425}Mn_{0.425}Co_{0.15})O_2$	1 = 2	2.8793(3)	14.282(3)	102.54(3)	0.2573(8)	0.072(8)	15.1	4.80
"$Li_{1.05}(Ni_{0.425}Mn_{0.425}Co_{0.15})_{0.95}O_{1.9}F_{0.1}$"	**1**	**2.8790(2)**	**14.282(2)**	**102.52(2)**	**0.2575(5)**	**0.063(6)**	**12.6**	**3.58**
	2	*2.8790(2)*	*14.282(1)*	*102.52(2)*	*0.2575(5)*	*0.073(6)*	*12.6*	*3.25*
"$Li_{1.10}(Ni_{0.425}Mn_{0.425}Co_{0.15})_{0.90}O_{1.8}F_{0.2}$"	**1**	**2.8785(2)**	**14.281(2)**	**102.48(2)**	**0.2579(2)**	**0.051(3)**	**13.2**	**4.85**
	2	*2.8785(2)*	*14.281(2)*	*102.48(2)*	*0.2579(6)*	*0.070(6)*	*13.0*	*4.59*

(*) **Hypothesis 1**: fluorine substitution for oxygen occurs; the chemical formula considered for the layered oxide is $Li_{1+z/2}(Ni_{0.425}Mn_{0.425}Co_{0.15})_{1-z/2}O_{2-z}F_z$.
Hypothesis 2: fluorine substitution for oxygen does not occur, fluorine is present as LiF in the material; the chemical formula considered for the layered oxide is $Li(Ni_{0.425}Mn_{0.425}Co_{0.15})O_2$.

Comparison of the cell parameters (a_{hex}, c_{hex} and volume) reported in Table 2 shows that within the 3σ standard deviation, their variation with fluorine substitution is not significant, despite ionic radii (1.33 and 1.40 Å, respectively) and electronegativities (4 and 3.5, respectively) significantly different for F^- and O^{2-}. The question that thus arises at this step is, is the fluorine substitution for oxygen effective? Structural refinements of the powder XRD data by the Rietveld method were performed considering first that fluorine substitution for oxygen is effective. The material structure was thus described by the following cation distribution: $(Li_{1-y}Ni_y)_{3b}(Li_{(z/2)}^{overlithiation}Li_yNi_{0.425(1-z/2)-y}Mn_{0.425(1-z/2)}Co_{0.15(1-z/2)})_{3a}(O_{2-z}F_z)_{6c}$, allowing an Li/Ni^{II} exchange in addition to the fluorination effect.

Then, for comparison, the analysis by the Rietveld method was also performed considering that fluorine substitution for oxygen did not occur and thus that the material was a mixture of two phases, the layered oxide $Li(Ni_{0.425}Mn_{0.425}Co_{0.15})O_2$ and LiF. In that case, the Rietveld analysis was performed considering the cation distribution $(Li_{1-y}Ni_y)_{3b}(Li_yNi_{0.425-y}Mn_{0.425}Co_{0.15})_{3a}(O_2)_{6c}$ for the α-$NaFeO_2$-type materials (again allowing partial Li/Ni^{II} exchange).

Whatever the hypothesis, the following constraints were considered:

(i) the oxygen, fluorine, lithium, cobalt, manganese and nickel total contents were fixed to the theoretical values, which are 0.425(1−z/2) for Ni distributed among the 3a and 3b sites, 0.425(1−z/2) for Mn in the 3a site, 0.15(1−z/2) for Co in the 3a site, (1+z/2) Li with at least (z/2) Li in the 3b site and finally 2−z and z for O and F, respectively, in the 6c site;
(ii) the three different sites (3b, 3a and 6c) were constrained to be fully occupied and
(iii) the atomic displacement parameters were constrained to be equal for all the ions present in a given site.

Note that the hypothesis of an Li/Ni^{II} exchange between the 3a and 3b sites was made in agreement with previous results obtained in our group for the $Li_{1+x}(Ni_{0.425}Mn_{0.425}Co_{0.15})_{1-x}O_2$ materials [11]. The results obtained from these two refinements for each composition are gathered in Table 2 in comparison with the ones obtained for the unfluorinated material. The refinement following the first hypothesis (i.e., effective fluorine substitution for oxygen) would imply that the nickel content in the interslab space (i.e., coming from the Li_{3a}/Ni^{II}_{3b} exchange) slightly decreases with increasing fluorine content (from 0.072(8) for $z = 0$ to 0.051(3) for $z = 0.2$). On the contrary, refinement following the second hypothesis would imply no variation in the Ni content in the interslab space (~0.07). Fig. 2 shows that, irrespective of the hypothesis considered, the quality of the Rietveld refinement was good. Using XRD only, it was therefore not possible to discriminate between these two hypotheses; indeed the electron density difference between fluorine and oxygen, as well as overlithiation, is compensated for by slight differences in the cation distribution between the 3a and 3b sites but again no significant difference is observed in the quality of the refinement and in the structural parameters between the two hypotheses.

3.2. ^{7}Li and ^{19}F MAS NMR spectroscopy analyses

^{7}Li and ^{19}F MAS NMR spectroscopy studies were performed to further characterize these materials, as this technique is very sensitive to both structural and electronic environments of the probed nucleus. Differences are thus expected for Li and F signals depending on their presence in the paramagnetic material $Li_{1+z/2}(Ni_{0.425}Mn_{0.425}Co_{0.15})_{1-z/2}O_{2-z}F_z$, characterized by single electrons for Ni and Mn ions that would interact with Li and F, or in a diamagnetic impurity such as LiF.

The ^{7}Li MAS NMR spectra obtained for these three materials are given in Fig. 3. The very broad signal corresponds to Li in the lamellar oxide material; its width (~600 ppm) results from dipolar interactions with the electronic spins of nickel and manganese, despite MAS. It is furthermore shifted to around 250 ppm due to the transfer of electron spin density from the transition metals to lithium (Fermi contact shift) [27]; the distribution of transition metals around Li leads to a distribution of Fermi contact shifts, which obviously also contributes to the residual width of the signal. The other signal is sharp and separated into spinning sidebands and its isotropic position is identical to that observed for Li in pure LiF (−1.4 ppm) (also reported in Fig. 3). This signal is clearly visible for the two samples

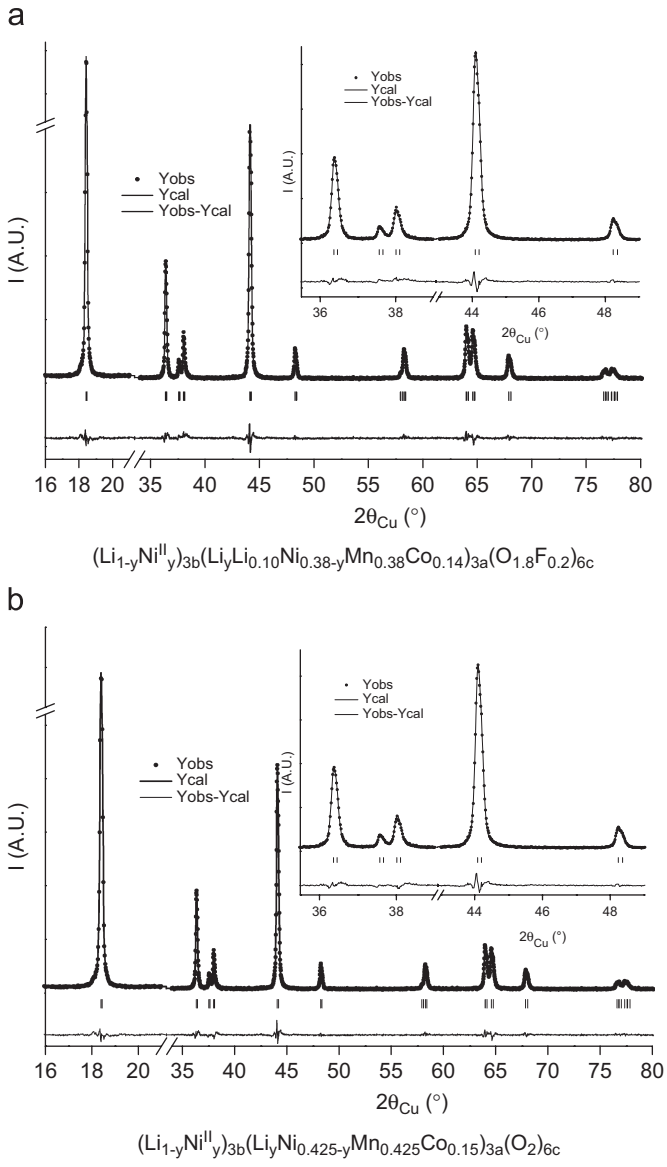

Fig. 2. Comparison of the experimental (•) and calculated (-) X-ray diffraction patterns considering (a) the formation of the $Li_{1+z/2}(Ni_{0.425}Mn_{0.425}Co_{0.15})_{1-z/2}O_{2-z}F_z$ phase ($z = 0.2$) and (b) a mixture "$0.9Li(Ni_{0.425}Mn_{0.425}Co_{0.15})O_2$+0.2LiF". The difference ($I_{obs}-I_{calc}$) is also given. The 90–120° (2θ) range is not represented to enlarge the figure.

containing fluorine, but traces of a similar signal also appear for the fluorine-free material. This corresponds to traces of Li_2CO_3 as commonly observed for that kind of materials due to the slight Li excess used for the synthesis [11], with an NMR chemical shift very close to 0 ppm.

Fig. 4 gives the ^{19}F MAS NMR spectra of $Li_{1+z/2}(Ni_{0.425}Mn_{0.425}Co_{0.15})_{1-z/2}O_{2-z}F_z$ materials ($z = 0$, 0.1, 0.2), with that of LiF. The broad signal observed for the three samples is an artefact from the probe as it contains PTFE in non-spinning parts. Note that the actual shape of this signal is somewhat sample-dependent since its proper phasing is not necessarily compatible with that of the signals from the samples. This makes it impossible in practice to subtract this signal from the experimental signal. An additional signal, sharp and separated into spinning sidebands, is observed in the fluorine-containing samples, with an isotropic position at −204 ppm. This signal has the same position as that of fluorine in LiF.

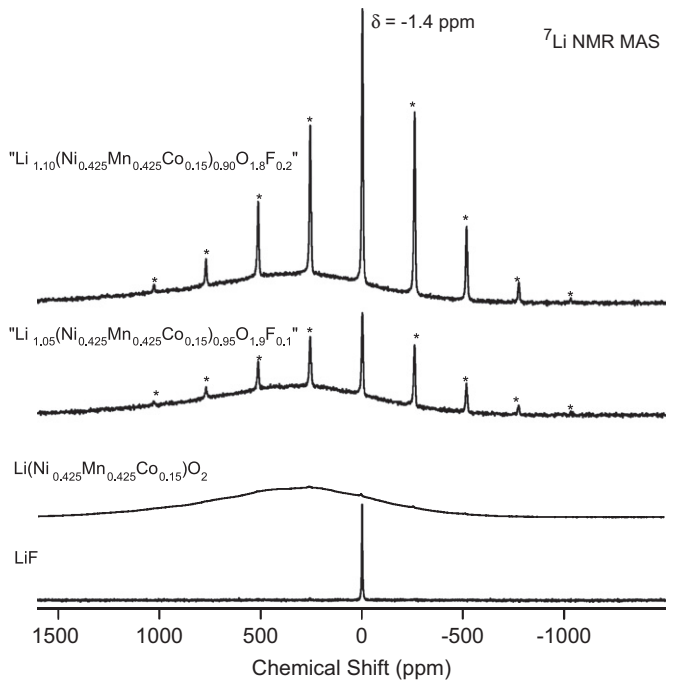

Fig. 3. ^7Li MAS NMR spectra (116.6 MHz, 30 kHz spinning; intensity scaled to the sample mass except for the LiF reference) of $Li_{1+z/2}(Ni_{0.425}Mn_{0.425}Co_{0.15})_{1-z/2}O_{2-z}F_z$ materials ($z = 0$, 0.1, 0.2) synthesized by coprecipitation. The weak 0 ppm signal for the unfluorinated sample corresponds to traces of lithium carbonate (see text). (*) spinning sidebands.

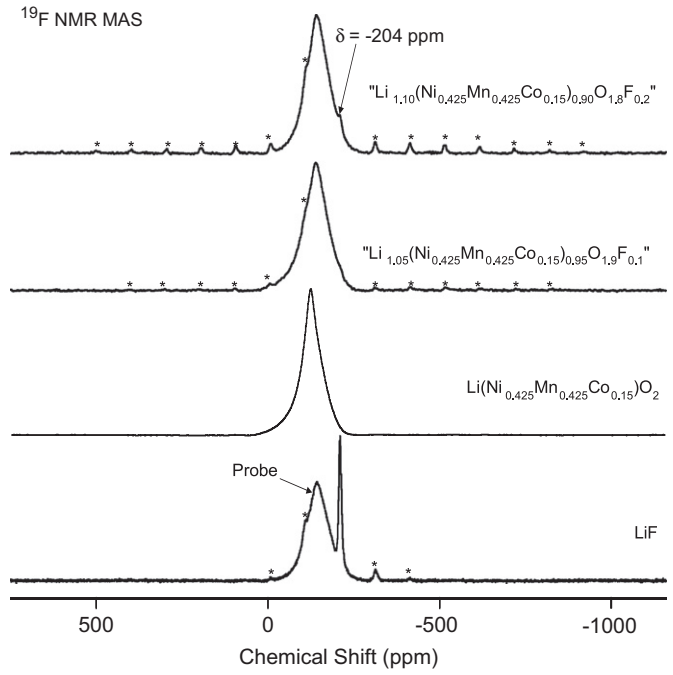

Fig. 4. ^{19}F MAS NMR spectra (282.4 MHz, 30 kHz spinning; intensity scaled to the sample mass except for the LiF reference) of $Li_{1+z/2}(Ni_{0.425}Mn_{0.425}Co_{0.15})_{1-z/2}O_{2-z}F_z$ materials ($z = 0$, 0.1, 0.2) synthesized by coprecipitation. (*) spinning sidebands.

An important feature from the NMR spectra is the striking difference in the line shape (spinning sidebands envelope) for the ^7Li and ^{19}F signals in the LiF standard compared with those of the sharp signals in the materials. Indeed, for both nuclei, the global width (number of spinning-side bands) is much larger for the fluorinated materials than for the LiF standard. The line shape of a

solid-state MAS NMR signal can be caused by anisotropies in chemical shift or (nuclear) dipolar interactions, as well as in quadrupolar interactions. However, the first two interactions can hardly lead to such a width (over 300 kHz for ^{7}Li and over 450 kHz for ^{19}F), and the shape is clearly not that of a quadrupolar interaction (no quadrupolar interaction is anyway possible for ^{19}F). The other possible origin for the global width is the (much stronger) dipolar interaction with electron spins [28,29]. This indicates that the Li and F nuclei responsible for the signals are rather close to the electronic spins of the layered oxide so that the through space dipolar interaction they exert leads to a broadening of the spinning sidebands envelope of the NMR signals, as observed for Li_2CO_3 in intimate contact with $Li(Ni,Co,Al)O_2$ by some of us [30]. However, it is important to note again that they have identical shifts to those for the LiF standard, showing that no electron spin is transferred to the Li and F nuclei, as would have been the case if they were present within the structure of the compound. The second hypothesis is thus supported by ^{7}Li and ^{19}F MAS NMR: fluorine substitution for oxygen did not occur; the material is a mixture of two phases, $Li(Ni_{0.425}Mn_{0.425}Co_{0.15})O_2$ and LiF, and LiF is present as a surface layer. Note that these results are in good agreement with those recently reported by Li et al. [26]: they showed using F(1*s*) XPS spectra and Ar ion etching that LiF added to $LiNi_{1/3}Mn_{1/3}Co_{1/3}O_2$ exists on the surface of the active material. In addition, an interesting feature is revealed by careful observation of Figs. 3 and 4: the more the LiF, the less intense the spinning sidebands are in relative magnitude. Indeed when the LiF amount increases, the LiF layer present on the surface of the paramagnetic material becomes thicker and as a consequence the amount of Li^+ ions relatively farther from the paramagnetic ions increases, leading to relatively narrower NMR line shapes, as was already discussed by some of us for an Li_2CO_3 layer that was present at the aged $Li(Ni,Co,Al)O_2$ surface [30].

Based on the particle size of the materials, the thickness of the LiF layer that should result if no LiF is incorporated in the materials is about 4–5 nm (in case of 0.9 $Li(Ni_{0.425}Mn_{0.425}Co_{0.15})O_2$+0.2 LiF), which is perfectly compatible with its non-observation by XRD.

4. Conclusion

In this work, "$Li_{1+z/2}(Ni_{0.425}Mn_{0.425}Co_{0.15})_{1-z/2}O_{2-z}F_z$" materials were prepared by coprecipitation. XRD patterns showed that all "$Li_{1+z/2}(Ni_{0.425}Mn_{0.425}Co_{0.15})_{1-z/2}O_{2-z}F_z$" materials were pure. Rietveld refinements of the XRD data showed similar structural parameters and cationic distributions irrespective of the fluorine amount and the hypothesis made (fluorine substitution for oxygen or not). ^{7}Li and ^{19}F MAS NMR revealed that there was no fluorine substitution for oxygen but a formation of LiF coating. The effect on the electrochemical performance of this coating, as well as that of similar ones obtained with different preparation conditions, will be reported elsewhere.

Acknowledgments

The authors wish to thank O. Jan (Saft) and Lydia Raison (ICMCB-CNRS) for technical assistance, Stéphane Levasseur (Umicore, Olen, Belgium) for fruitful discussions, and Région Aquitaine and Saft for financial support.

References

[1] J.P. Pérès, C. Delmas, A. Rougier, M. Broussely, F. Perton, P. Biensan, P. Willmann, J. Phys. Chem. Solids 57 (1996) 1057.
[2] M. Broussely, F. Perton, P. Biensan, J.M. Bodet, J. Labat, A. Lecerf, C. Delmas, A. Rougier, J.P. Pérès, J. Power Sources 54 (1995) 109.
[3] J.R. Dahn, E.W. Fuller, M. Obrovac, U. Von Sacken, Solid State Ionics 69 (1994) 265.
[4] T. Ohzuku, A. Ueda, M. Kouguchi, J. Electrochem. Soc. 142 (1995) 4033.
[5] H. Arai, S. Okada, Y. Sakurai, J. Yamaki, Solid State Ionics 109 (1998) 295.
[6] M. Guilmard, L. Croguennec, D. Denux, C. Delmas, Chem. Mater. 15 (2003) 4476.
[7] M. Broussely, P. Blanchard, P. Biensan, J.P. Planchat, K. Nechev, R.J. Staniewicz, J. Power Sources 119 (2003) 859.
[8] T. Ohzuku, Y. Makimura, Chem. Lett. 642 (2001).
[9] B.J. Hwang, Y.W. Tsai, D. Carlier, G. Ceder, Chem. Mater. 15 (2003) 3676.
[10] D. Li, T. Muta, L. Zhang, M. Yoshio, H. Noguchi, J. Power Sources 132 (2004) 150.
[11] N. Tran, L. Croguennec, C. Labrugère, C. Jordy, P. Biensan, C. Delmas, J. Electrochem. Soc. 153 (2) (2006) A261.
[12] N. Tran, L. Croguennec, C. Jordy, P. Biensan, C. Delmas, Solid State Ionics 176 (2005) 1539.
[13] K.M. Shaju, G.V. Subba Rao, B.V.R. Chowdari, Electrochem. Acta 48 (2002) 145.
[14] W.S. Yoon, C.P. Grey, M. Balasubramanian, X.Q. Yang, J. McBreen, Chem. Mater. 15 (2003) 3161.
[15] Z. Chen, Y.-K. Sun, K. Amine, J. Electrochem. Soc. 153 (2006) A1818.
[16] S.K. Hu, T.C. Chou, B.J. Hwang, G. Ceder, J. Power Sources 160 (2006) 1287.
[17] J. Guo, L.F. Jiao, H.T. Yuan, L.Q. Wang, H.X. Li, M. Zhang, Y.M. Wang, Electrochem. Acta 51 (2006) 6275.
[18] G.H. Kim, S.T. Myung, H.S. Kim, Y.K. Sun, Electrochem. Acta 51 (2006) 2447.
[19] M. Kageyama, D. Li, K. Kobayabawa, Y. Sato, J. Power Sources 157 (2006) 494.
[20] S.T. Myung, K. Izumi, S. Komaba, H. Yashiro, H.J. Bang, Y.K. Sun, N. Kumagai, J. Phys. Chem. 111 (2007) 4061.
[21] S. Jouanneau, J.R. Dahn, J. Electrochem. Soc. 151 (2004) A1749.
[22] G.H. Kim, S.T. Myung, H.J. Bang, J. Prakash, Y.K. Sun, Electrochem. Solid State Lett. 7 (2004) A477.
[23] G.H. Kim, M.H. Kim, S.T. Myung, Y.K. Sun, J. Power Sources 146 (2005) 602.
[24] S.U. Woo, B.C. Park, C.S. Yoon, S.T. Myung, J. Prakash, Y.K. Sun, J. Electrochem. Soc. 154 (2007) A649.
[25] S.H. Kang, K. Amine, J. Power Sources 146 (2005) 654.
[26] D. Li, Y. Sasaki, K. Kobayabawa, H. Noguchi, Y. Sato, Electrochem. Acta 52 (2006) 643.
[27] C. Marichal, J. Hirschinger, P. Granger, M. Ménétrier, A. Rougier, C. Delmas, Inorg. Chem. 34 (1995) 1773.
[28] C.P. Grey, N. Dupré, Chem. Rev. 104 (2004) 4493.
[29] C. Chazel, M. Ménétrier, L. Croguennec, C. Delmas, Magn. Reson. Chem. 43 (2005) 849.
[30] M. Ménétrier, C. Vaysse, L. Croguennec, C. Delmas, C. Jordy, F. Bonhomme, P. Biensan, Electrochem. Solid State Lett. 7 (2004) A140.